An efficient stochastic algorithm for studying coagulation dynamics and gelation phenomena

Andreas Eibeck and Wolfgang Wagner

Weierstrass Institute for Applied Analysis and Stochastics
Mohrenstraße 39, D–10117 Berlin, Germany
email: eibeck@wias-berlin.de, wagner@wias-berlin.de

Abstract. A new class of efficient stochastic algorithms for the numerical treatment of coagulation processes is proposed. The algorithms are based on the introduction of fictitious jumps combined with an acceptance-rejection technique for distributions depending on particle size. The increased efficiency is demonstrated by numerical experiments. In particular, gelation phenomena are studied.

Contents

1. Introduction

The **continuous coagulation equation**

$$\frac{\partial}{\partial t} c(t,x) = \frac{1}{2}\int_0^x K(x-y,y)\, c(t,x-y)\, c(t,y)\, dy \;-\; \int_0^\infty K(x,y)\, c(t,x)\, c(t,y)\, dy \quad (1.1)$$

with initial condition

$$c(0,x) = c_0(x) \ge 0 \quad (1.2)$$

describes the time evolution of the average concentration of particles of size $x > 0$. Here the non-negative and symmetric function $K(x,y)$ denotes the coagulation rate of clusters of size x and y . According to (1.1), the concentration $c(x,t)$ can increase by coagulation of clusters of size $y < x$ and $x - y$ (first term) and decrease by coagulation of an x-cluster with a cluster of any size y (second term).

If the clusters only can take sizes $k = 1, 2, \dots$, then the coagulation dynamics is governed by a discrete version of equation (1.1), where all integrals are replaced by sums. The **discrete coagulation equation**

$$\frac{\partial}{\partial t} c(t,k) = \frac{1}{2}\sum_{j=1}^{k-1} K(k-j,j)\, c(t,k-j)\, c(t,j) - \sum_{j=1}^{\infty} K(k,j)\, c(t,k)\, c(t,j) \quad (1.3)$$

was first published in [22] and is referred to as Smoluchowski's coagulation equation. Both the continuous and the discrete equation have a wide range of applications, e.g., in astrophysics, biology, chemistry and meteorology (see the survey papers [6] and [2]).

Stochastic particle systems related to the coagulation equation were introduced by several authors (cf. [17], [10], [16]). They are of the form

$$x_i(t)\,, \quad i = 1, \dots, n(t)\,, \qquad t \ge 0\,, \quad (1.4)$$

where $x_i(t)$ represents the size of particle i at time t , and $n(t)$ is the number of particles in the system. The initial system consisting of a large number $n(0)$ of particles is supposed to approximate the initial condition (1.2). A random dynamics is defined such that the system at later times approximates the solution to equation (1.1). The stochastic approach to coagulation was reviewed in [2]. Recently, rigorous results concerning the weak law of large numbers for the relevant stochastic particle systems with general kernels have been obtained (see [2, Problem 10(a)], [12], [13], [14], [18], [7]). Beside the derivation of the coagulation equation, stochastic particle systems play a significant role in numerical algorithms for that equation (see [11], [5]). We refer to [20] for a survey on **Monte Carlo methods**, and to [19] concerning recent applications.

The **purpose of this paper** is to introduce a new class of efficient stochastic algorithms for the numerical treatment of the coagulation equation. The idea was mentioned in [7], where we studied the convergence problem. Here we give a detailed description of the numerical procedure and apply it to the investigation of some interesting phenomena.

The paper is organized as follows. In **Section 2** we describe the new class of algorithms. Markov processes with fictitious jumps are introduced, which are based on appropriate majorant kernels. An efficient acceptance-rejection procedure for the generation of the relevant probability distributions is proposed. In **Section 3** we apply the numerical technique to the study of coagulation dynamics. For several coagulation kernels we investigate approximation properties and gelation phenomena. In **Section 4** we discuss the results and mention some directions for further study.

2. Description of the algorithm

2.1. Markov processes with fictitious jumps

We introduce a **sequence of jump processes**

$$U^N(t)\,, \qquad t \ge 0\,, \qquad N = 1, 2 \dots\,, \tag{2.1}$$

taking values in the space of discrete measures

$$\mathcal{S}^N = \left\{ p = \frac{1}{N} \sum_{i=1}^{n} \delta_{x_i}\,, \quad x_i > 0\,, \quad n = 1, 2, \dots \right\}.$$

For $\Phi \in C_b(\mathcal{S}^N)$ the infinitesimal generator is defined as

$$\mathcal{K}^N \Phi(p) = \frac{1}{2N} \sum_{1 \le i \ne j \le n} \Big[\Phi(J(p,i,j)) - \Phi(p) \Big] K(x_i, x_j)\,, \qquad p \in \mathcal{S}^N\,, \tag{2.2}$$

where

$$J(p,i,j) = p + \frac{1}{N} (\delta_{x_i + x_j} - \delta_{x_i} - \delta_{x_j})\,. \tag{2.3}$$

The **initial condition** is assumed to be deterministic and such that (cf. (1.2))

$$\lim_{N \to \infty} \int_0^\infty \varphi(x)\, U^N(0, dx) = \int_0^\infty \varphi(x)\, c_0(x)\, dx\,, \tag{2.4}$$

for a sufficiently wide class of test functions φ. In particular, for $\varphi = 1$, one obtains

$$n(0) \quad \sim \quad N \int_0^\infty c_0(x)\, dx\,. \tag{2.5}$$

Convergence of $U^N(t)$ to the solution of a measure-valued version of equation (1.1) was studied in [18].

We will describe a **class of simulation algorithms** related to the stochastic systems determined by (2.2)-(2.4). Note that the infinitesimal generator (2.2) does not change if one adds terms of the form

$$\frac{1}{2N} \sum_{1 \le i \ne j \le n} \Big[\Phi(p) - \Phi(p) \Big] \Big[\hat{K}(x_i, x_j) - K(x_i, x_j) \Big]\,,$$

where $\hat{K}$ is an appropriate function such that

$$K(x,y) \;\leq\; \hat{K}(x,y)\,, \qquad x,y>0\,. \tag{2.6}$$

However, this introduction of artificial "fictitious" jumps (cf., e.g., [8, p. 163]) provides a variety of ways to generate trajectories of the process. The efficiency of the simulation procedure depends on the choice of the **majorant kernel** $\hat{K}$.

We first describe the **general simulation procedure** before turning to some special cases.

0. Generate the initial state $U^N(0)=p\in\mathcal{S}^N$.

1. Wait an exponentially distributed **time step** τ with parameter

$$\hat{\varrho}(p)=\frac{1}{2N}\sum_{1\leq i\neq j\leq n}\hat{K}(x_i,x_j)\,. \tag{2.7}$$

2. Choose a pair i,j according to the **index distribution**

$$\frac{\hat{K}(x_i,x_j)}{2N\,\hat{\varrho}(p)}\,, \qquad 1\leq i\neq j\leq n\,. \tag{2.8}$$

3. With probability

$$\frac{K(x_i,x_j)}{\widehat{K}(x_i,x_j)}\,, \tag{2.9}$$

replace p by the new state $J(p,i,j)$, i.e. remove the clusters x_i and x_j and add the cluster x_i+x_j . Otherwise, the interaction is **fictitious**, i.e. nothing changes.

4. Go to step 1.

Note the **mass conservation** property

$$\int_0^\infty x\,U^N(t,dx) \;=\; \int_0^\infty x\,U^N(0,dx)\,, \qquad t\geq 0\,, \tag{2.10}$$

which is a consequence of (2.3).

The **special case**

$$\hat{K}(x,y)=K(x,y)\,, \qquad x,y>0\,, \tag{2.11}$$

corresponds to the straightforward simulation of the process (see [11], [5]). Here the time steps, having the average value $\hat{\varrho}(p)^{-1}$, are as large as possible, and no fictitious jumps occur. However, the calculation of (2.7) and the generation of the distribution (2.8) are very time consuming if n is large and K has a complicated structure.

In the **special case**

$$\hat{K}(x,y)=K_{max}(p)=\max_{i,j=1,\ldots,n}K(x_i,x_j)\,, \qquad x,y>0\,, \tag{2.12}$$

one obtains a simulation procedure (see, e.g., [11], [9] , [20]) which is in some sense opposite to the simulation corresponding to (2.11). Namely, the calculation of (2.7) and the generation of the distribution (2.8) are extremely simple. Indeed, the waiting time parameter takes the form

$$\hat{\varrho}(p) = K_{max}(p)\,\frac{n\,(n-1)}{2N}\,, \tag{2.13}$$

and the index distribution is uniform. However, the time steps are very small, and many fictitious jumps occur, if K is unbounded and clusters of significantly different sizes are contained in the system.

2.2. Choice of the majorant kernel

We consider the majorant kernel (cf. (2.6))

$$\hat{K}(x,y) = C\,x^{\varepsilon_1}\,y^{\varepsilon_2}\,, \qquad C>0\,, \quad \varepsilon_1\,,\varepsilon_2 \ge 0\,. \tag{2.14}$$

The **waiting time parameter** (2.7) takes the form

$$\hat{\varrho}(p) = \frac{C}{2N}\sum_{i=1}^{n} x_i^{\varepsilon_1} \sum_{j=1,\ldots,n,\,j\neq i} x_j^{\varepsilon_2} = \frac{C}{2N}\left[\sum_{i=1}^{n} x_i^{\varepsilon_1}\sum_{j=1}^{n} x_j^{\varepsilon_2} - \sum_{i=1}^{n} x_i^{\varepsilon_1+\varepsilon_2}\right]. \tag{2.15}$$

The **index distribution** (2.8) is generated using the **acceptance-rejection technique**. To this end the events $i=j$ are added to the state space and the zero probability for $i=j$ in (2.8) is replaced by an appropriate term proportional to $x_i^{\varepsilon_1}\,x_j^{\varepsilon_2}$. Then the index distribution takes the form

$$\frac{x_i^{\varepsilon_1}}{\sum_{l=1}^{n} x_l^{\varepsilon_1}}\,\frac{x_j^{\varepsilon_2}}{\sum_{l=1}^{n} x_l^{\varepsilon_2}}\,, \qquad i,j=1,\ldots,n\,,$$

so that the indices i and j are independent. The simulation procedure is as follows.

1. Generate i according to

$$\frac{x_i^{\varepsilon_1}}{\sum_{l=1}^{n} x_l^{\varepsilon_1}}\,, \qquad i=1,\ldots,n\,. \tag{2.16}$$

2. Generate j according to

$$\frac{x_j^{\varepsilon_2}}{\sum_{l=1}^{n} x_l^{\varepsilon_2}}\,, \qquad j=1,\ldots,n\,. \tag{2.17}$$

3. If $i=j$ then go to step 1.

More general majorant kernels of the form

$$\hat{K}(x,y) = \hat{K}_1(x,y) + \ldots + \hat{K}_L(x,y)\,, \qquad L \ge 2\,, \tag{2.18}$$

can be used. The **waiting time parameter** (2.7) is

$$\hat{\varrho}(p) = \hat{\varrho}_1(p) + \ldots + \hat{\varrho}_L(p)\,,$$

where

$$\hat{\varrho}_k(p) = \frac{1}{2N} \sum_{1 \le i \ne j \le n} \hat{K}_k(x_i, x_j)\,, \qquad k = 1, \ldots, L\,.$$

The **index distribution** (2.8) takes the form

$$\sum_{k=1}^{L} \frac{\hat{\varrho}_k(p)}{\hat{\varrho}(p)} \, \frac{\hat{K}_k(x_i, x_j)}{2N\,\hat{\varrho}_k(p)}\,, \qquad 1 \le i \ne j \le n\,.$$

Thus, one first chooses a number k according to the probabilities

$$\frac{\hat{\varrho}_k(p)}{\hat{\varrho}(p)}\,, \qquad k = 1, \ldots, L\,, \tag{2.19}$$

and then generates i, j according to the distribution

$$\frac{\hat{K}_k(x_i, x_j)}{2N\,\hat{\varrho}_k(p)}\,, \qquad 1 \le i \ne j \le n\,.$$

Example 2.1 *Consider the case*

$$\hat{K}(x, y) = C\,(x + y)\,, \qquad x, y > 0\,. \tag{2.20}$$

This kernel has the form (2.18). One obtains the waiting time parameter

$$\hat{\varrho}(p) \;=\; C\,m_1\,(n-1)\,, \tag{2.21}$$

where $m_1 = \frac{1}{N}\sum_{i=1}^{n} x_i$ *. Note that*

$$m_1 \;=\; \int_0^\infty x\,U^N(0, dx) \tag{2.22}$$

according to the mass conservation property (2.10). The index i is generated according to the distribution

$$\frac{x_i}{N\,m_1}\,, \qquad i = 1, \ldots, n\,. \tag{2.23}$$

The index j is generated uniformly on the set $\{k = 1, \ldots, n\,, \quad k \ne i\}$ avoiding the acceptance rejection step. The random choice according to (2.19) is omitted, since the result of the interaction (2.3) does not depend on the order of the indices.

Example 2.2 *Consider the case*

$$\hat{K}(x, y) = C\,x\,y\,, \qquad x, y > 0\,. \tag{2.24}$$

This kernel has the form (2.14) with $\varepsilon_1 = \varepsilon_2 = \varepsilon$. From (2.15) one obtains the waiting time parameter

$$\hat{\varrho}(p) \;=\; \frac{C\,N\,m_1^2}{2} - \frac{C}{2\,N}\sum_{i=1}^{n} x_i^2\,,$$

where m_1 is defined in (2.22). Note that $n = 1$ implies $x_1 = N\,m_1$ and $\hat{\varrho}(p) = 0$. The indices i, j are generated independently, according to the distribution (2.23). They are rejected if $i = j$.

2.3. Generation of a size dependent distribution

In order to generate the distribution

$$\frac{x_j^\varepsilon}{\sum_{l=1}^n x_l^\varepsilon}\,, \qquad j=1,\ldots,n\,, \qquad \varepsilon>0\,, \tag{2.25}$$

efficiently (cf. (2.16), (2.17), (2.23)), we introduce a **group structure** of the particle system $(x_i)_{i=1}^n$. The particles are organized in γ groups, i.e. their sizes are denoted by

$$y_{j,k}\,, \qquad j=1,\ldots\gamma\,, \quad k=1,\ldots,\alpha_j\,,$$

so that

$$b_{j-1}<y_{j,k}\le b_j\,, \qquad \forall j=1,\ldots\gamma\,, \quad k=1,\ldots,\alpha_j\,,$$

where

$$0=:b_0<b_1<\ldots<b_\gamma \tag{2.26}$$

and (cf. (2.22))

$$N\,m_1\le b_\gamma\,. \tag{2.27}$$

Note that $N\,m_1$ is the upper bound for the particle size.

The distribution (2.25) is rewritten as

$$\frac{y_{j,k}^\varepsilon}{c}\,, \qquad j=1,\ldots\gamma\,, \quad k=1,\ldots,\alpha_j\,, \tag{2.28}$$

where the normalizing constant is

$$c=\sum_{l=1}^n x_l^\varepsilon=\sum_{j=1}^\gamma\sum_{k=1}^{\alpha_j} y_{j,k}^\varepsilon\,. \tag{2.29}$$

The representation (2.28), (2.29) suggests the following simulation procedure using the **acceptance-rejection technique**.

1. Choose the **group index** according to the probabilities

$$P_j=\frac{1}{c}\sum_{k=1}^{\alpha_j} y_{j,k}^\varepsilon\,, \qquad j=1,\ldots,\gamma\,. \tag{2.30}$$

2. Choose the **particle index** $k=1,\ldots,\alpha_j$ uniformly within the group j .

3. The particle index is **accepted** with probability

$$\frac{y_{j,k}^\varepsilon}{b_j^\varepsilon}\,. \tag{2.31}$$

   Otherwise, go to step 2.

With

$$b_j = \beta^{j-1}\,, \qquad j = 1, 2, \dots\,,$$

where $\beta > 1$, the **acceptance probability** (2.31) for groups $j \geq 2$ is bounded from below by

$$\frac{1}{\beta^{\varepsilon}}\,. \tag{2.32}$$

The necessary **number of groups** $\gamma = \gamma(N, \beta)$ is obtained from the estimate (cf. (2.27))

$$\beta^{\gamma-2} < N\, m_1 \leq \beta^{\gamma-1} \qquad \text{or} \qquad \gamma - 2 < \frac{\log(N\, m_1)}{\log \beta} \leq \gamma - 1\,. \tag{2.33}$$

Remark 2.3 *For $\beta \searrow 1$, the number of rejections decreases according to (2.32), leading to higher efficiency. On the other hand the number of groups γ increases according to (2.33), and generating the distribution (2.30) becomes more and more time consuming.*

3. Applications to coagulation dynamics

The jump process (2.1) is represented by a system of particles (1.4). Functionals of the solution of equation (1.1) are approximated as

$$\int_0^\infty \varphi(x)\, c(t,x)\, dx \;\sim\; \int_0^\infty \varphi(x)\, U^N(t, dx) = \frac{1}{N} \sum_{i=1}^{n(t)} \varphi(x_i(t))\,, \qquad t \geq 0\,, \tag{3.1}$$

where φ is some test function. Many functionals of interest are expressed via **moments** of the solution

$$m_\delta(t) = \int_0^\infty x^\delta\, c(t,x)\, dx\,, \qquad \delta \geq 0\,. \tag{3.2}$$

In particular, $m_0(t)$ is the **total concentration** of particles, $m_1(t)$ is the **total mass** of the system, and

$$S(t) = \frac{m_1(t)}{m_0(t)} = \frac{\int_0^\infty x\, c(t,x)\, dx}{\int_0^\infty c(t,x)\, dx}$$

is the **average particle size**. Moments (3.2) are approximated according to (3.1) as

$$m_\delta(t) \;\sim\; \frac{1}{N} \sum_{i=1}^{n(t)} x_i(t)^\delta\,. \tag{3.3}$$

In the following we restrict our considerations to the **discrete equation** (1.3) with **monodisperse initial condition**

$$c(0,1) = 1\,, \qquad c(0,k) = 0\,, \quad k = 2, 3, \dots\,. \tag{3.4}$$

In this case some explicit solutions are available (cf., e.g., [2, Section 2.2]). This is convenient for validating the algorithm. The solution represents the concentration of particles of given size and is approximated as

$$c(t,k) \quad \sim \quad \frac{1}{N}\,\#\{i\,:\,x_i(t)=k\}\,, \qquad k=1,2,\ldots\,, \quad t\ge 0\,. \tag{3.5}$$

According to (3.4) we start with the particle system (cf. (2.4), (2.5))

$$x_i(0)=1\,, \qquad i=1,\ldots,N\,. \tag{3.6}$$

Confidence bands with confidence level 99.9% are constructed using R independent runs, where $R\,N=10^7$.

3.1. Explicit solutions

The **special case** of constant coagulation rate and initial condition (3.4) was solved in the original paper [22]. For

$$K(i,j)=1$$

one obtains

$$c(t,k)=\frac{4}{(2+t)^2}\left(\frac{t}{2+t}\right)^{k-1}, \qquad t\ge 0\,, \quad k=1,2,\ldots\,,$$

and

$$m_0(t)=\frac{2}{2+t}\,, \qquad m_1(t)=1\,, \qquad m_2(t)=1+t\,, \qquad t\ge 0\,.$$

In the **special case**

$$K(i,j)=i+j \tag{3.7}$$

one obtains

$$c(t,k)=e^{-t}\,\frac{k^{k-1}}{k!}\,(1-e^{-t})^{k-1}\,e^{-k(1-e^{-t})}\,, \qquad t\ge 0\,, \quad k=1,2,\ldots\,, \tag{3.8}$$

and

$$m_0(t)=e^{-t}\,, \qquad m_1(t)=1\,, \qquad m_2(t)=e^{2t}\,, \qquad t\ge 0\,.$$

In the **special case**

$$K(i,j)=i\,j \tag{3.9}$$

the global solution of equation (1.3) is given by (cf. [15, Th.2.2])

$$c(t,k) \quad = \quad \begin{cases} \frac{k^{k-2}}{k!}\,t^{k-1}\,\exp(-kt)\,, & \text{if} \quad 0\le t\le 1\,,\\[2ex] \frac{k^{k-2}}{k!}\,\exp(-k)\,t^{-1}\,, & \text{if} \quad 1<t\,. \end{cases} \tag{3.10}$$

For the total concentration one obtains

$$m_0(t) \quad = \quad \begin{cases} 1 - \frac{t}{2}\,, & \text{if} \quad 0 \le t \le 1\,, \\ \frac{1}{2t}\,, & \text{if} \quad 1 < t\,. \end{cases}$$

The total mass behaves like

$$m_1(t) \quad = \quad \begin{cases} 1\,, & \text{if} \quad 0 \le t \le 1\,, \\ \frac{1}{t}\,, & \text{if} \quad 1 < t\,, \end{cases} \tag{3.11}$$

and the second moment takes the form

$$m_2(t) \quad = \quad \frac{1}{1-t}\,, \qquad 0 \le t < 1\,.$$

Remark 3.1 *Note that the function*

$$\tilde{c}(t,x) = \mu\, c(\mu\, \sigma\, t, x)\,, \qquad t \ge 0\,, \quad x > 0\,, \qquad \mu, \sigma \ge 0\,,$$

solves equation (1.1) with the kernel $\tilde{K} = \sigma\, K$ *instead of* K *and initial condition* $\tilde{c}_0 = \mu\, c_0$ *instead of* c_0 .

3.2. Examples of coagulation kernels

In our numerical investigations we use the following three coagulation kernels.

The **first kernel** is

$$K_1(i,j) = \frac{1}{4}\,(i^{\frac{1}{3}} + j^{\frac{1}{3}})^3\,. \tag{3.12}$$

This kernel is of practical importance in connection with coagulation processes in turbulent flows (cf. [19]). Note that

$$K_1(u\,i, u\,j) = u\, K_1(i,j)\,, \qquad \forall u > 0\,. \tag{3.13}$$

According to

$$\frac{1}{4}\,(i+j) \le K_1(i,j) \le i+j\,,$$

the majorant kernel (2.20) is used (cf. (2.6)).

The **second kernel** is

$$K_2^{(a)}(i,j) = \frac{2\, i^a\, j^a}{(i+j)^a - i^a - j^a}\,, \qquad a \in (1,2]\,. \tag{3.14}$$

For this kernel an explicit formula for some moments is known (see, e.g., [1]), namely

$$m_a(t) = \frac{1}{1-t}\,, \qquad t \in [0,1)\,. \tag{3.15}$$

Note that

$$K_2^{(a)}(u\,i, u\,j) = u^a\, K_2^{(a)}(i,j)\,, \qquad \forall u > 0\,. \tag{3.16}$$

According to

$$K_2^{(a)}(i,j) \leq \frac{2}{2^a - 2}\, i\, j\,, \tag{3.17}$$

the majorant kernel (2.24) is used. In case $a = 2$ there is equality in (3.17).

The **third kernel** is

$$K_3^{(a)}(i,j) = i^a\, j^a\,, \qquad a \in (0.5, 1]\,. \tag{3.18}$$

This kernel has the form (2.14) and the (trivial) majorant kernel (2.11) will be used. Note that

$$K_3^{(a)}(u\,i, u\,j) = u^{2a}\, K_3^{(a)}(i,j)\,, \qquad \forall u > 0\,. \tag{3.19}$$

3.3. Approximation properties

To get a first impression of how the algorithm works, we consider the linear kernel (3.7). Here one takes $\hat{K} = K$ (cf. Example 2.1) and no fictitious jumps occur. Using a particle number $N = 10^6$ we calculate the solution $c(t,k)$ and some integrated functionals of the form

$$C(t,k) = \sum_{l \geq k} c(t,l)\,, \tag{3.20}$$

for different values of size k. The results are displayed in **Figure 1**, where the analytic curves (cf. (3.8)) are represented by solid lines and the confidence bands by dotted lines. The components of the solution $c(t,k)$ are sufficiently well approximated up to $k = 200$. The time instants where these functions take their maximum can be clearly detected. The fluctuations grow with increasing size, since the values of the functionals become very small. Functionals of the form (3.20) are well approximated even up to $k = 2000$.

Next we compare the solution for the kernel (3.12) with the solution for the linear kernel (3.7). Since at time zero both kernels are identical in case of initial configuration (3.6), it is of interest to study the deviation of both solutions during the time evolution. The confidence bands for the solution corresponding to the kernel (3.12) are shown in **Figure 2** and compared with the exact solutions for the kernel (3.7) (solid lines).

Finally we illustrate the convergence with respect to the initial particle number N for the kernel (3.14) with $a = 1.5$. We calculate the behaviour of the moment $m_{1.5}(t)$ on the time interval $[0,1]$ via (3.3) and compare the results with the explicit expression (3.15). The results are displayed in **Figure 3**. For $N = 10^4$ the exact solution (solid line) is almost indistinguishable from the confidence band up to the time $t = 0.8$. For larger N the exact solution leaves the confidence band at later times.

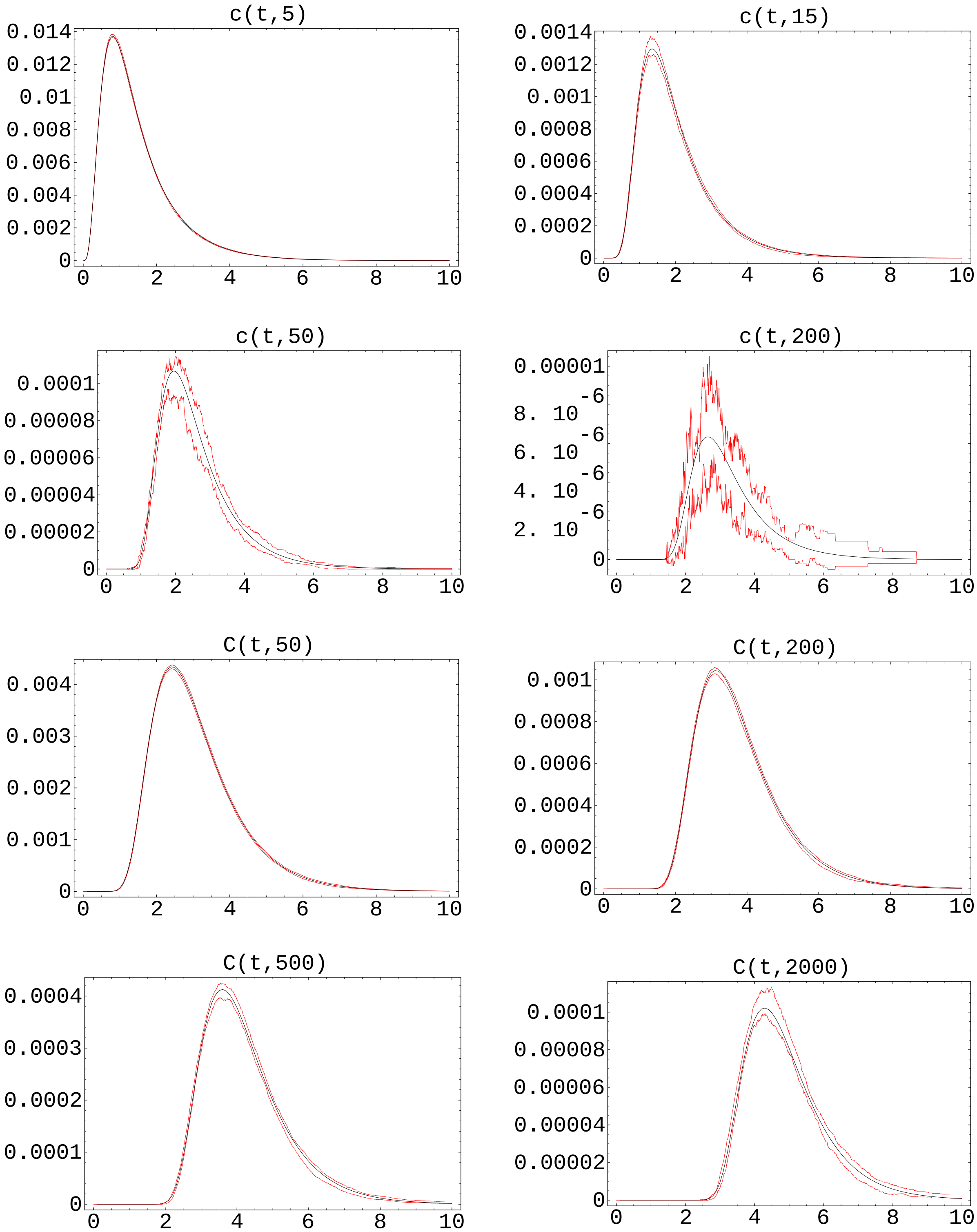

Figure 1: Concentration functionals $c(t, k)$ and $C(t, k)$ for the linear kernel (3.7)

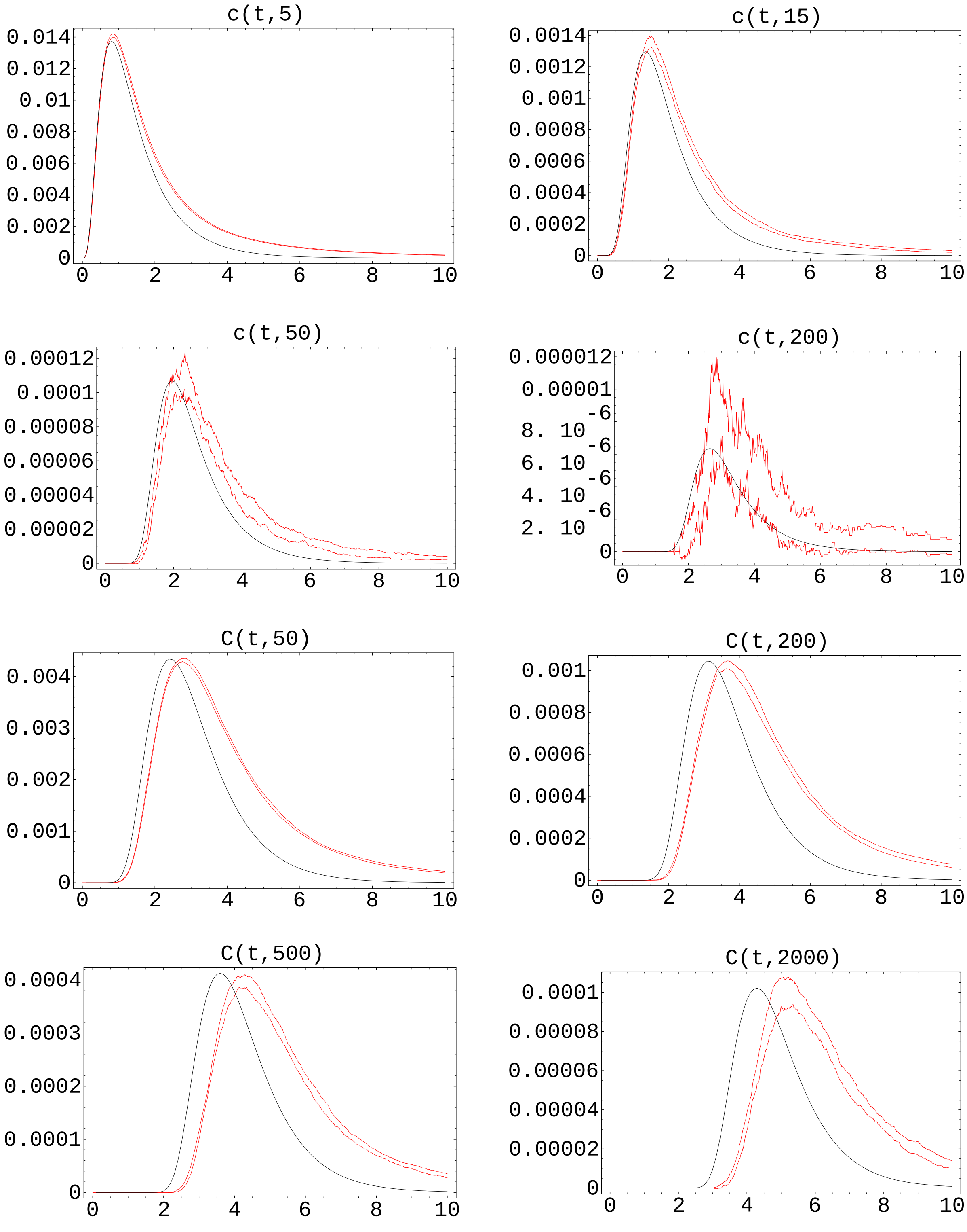

Figure 2: Concentration functionals $c(t,k)$ and $C(t,k)$ for the kernel (3.12)

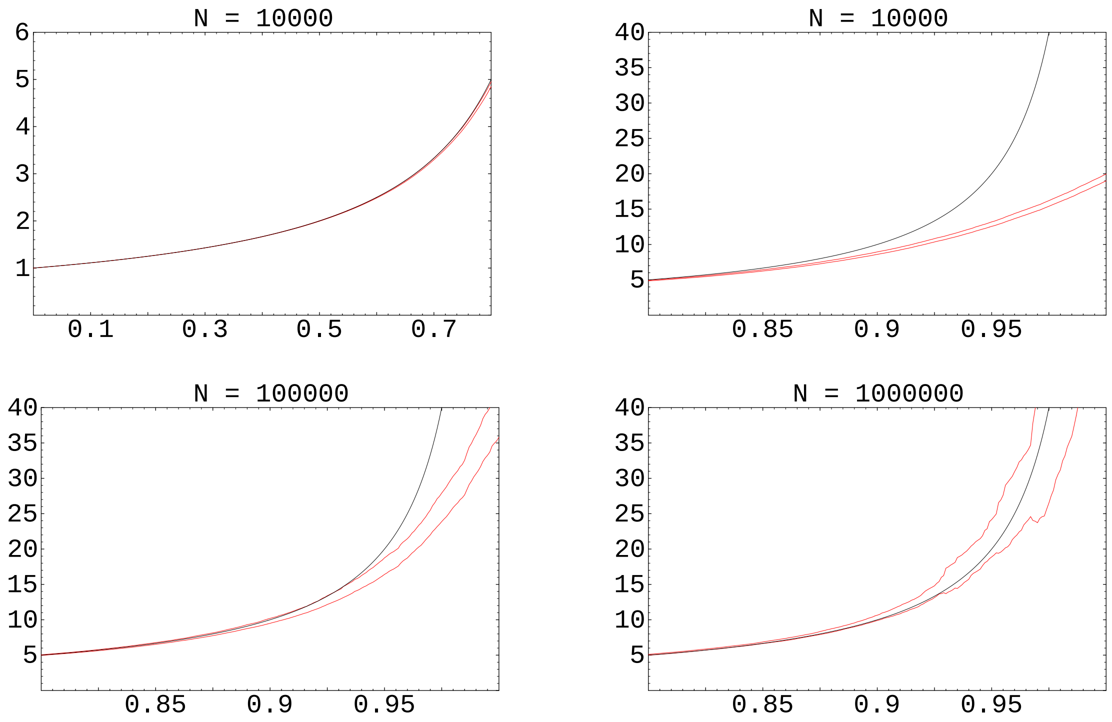

Figure 3: Moment (3.15) for the kernel for the kernel (3.14) with $a = 1.5$

3.4. Gelation phenomena

In the case of the multiplicative kernel (3.9) the total mass is not conserved (cf. (3.11)). This effect is interpreted as formation of infinite clusters and called **gelation** (cf. [2], [14]). Our test kernels (3.12), (3.14) and (3.18) are homogeneous (cf. (3.13), (3.16), (3.19)) with exponents 1, a and $2a$, respectively. Homogeneous kernels with exponents greater than 1 are expected to be gelling (see [2, Section 2.3]).

In the **finite particle system** (1.4) the total mass is always conserved (cf. (2.10)). An appropriate indicator for gelation is the behaviour of the **largest component** $M_1(t)$ in the system. For the multiplicative kernel (3.9), the particle with the largest size is of order N after the **gelation time**

$$t_g = \inf\{t > 0 \; : \; m_1(t) > 0\}$$

and of lower order before t_g (see [2, Section 4.4]). The quantity $\frac{M_1(t)}{N}$ is convenient for studying general gelling kernels (see [2, Section 5.2]) using the stochastic algorithm. Note that $\frac{M_1(t)}{N} \in [0,1]$ and $M_1(t) \leq M_1(t')$, $t \leq t'$.

As an example we consider the kernel (3.18) with $a = 0.7, 0.8, 0.9, 1.0$. The curves for the quantity $\frac{M_1(t)}{N}$ with $N = 10^4, 10^5, 10^6$ are shown by dotted, dashed and solid lines, respectively, in **Figure 4**. The behaviour of the second largest component divided by N for $N = 10^4$ (dotted), $N = 10^5$ (dashed) and $N = 10^6$ (solid) is shown in **Figure 5**. For comparison the curves for both components and $N = 10^6$ are displayed together on the same scale in **Figure 6**, where, in addition, the dashed lines represent the total concentration $m_0(t)$. Analogous results for the kernel (3.14) with $a = 1.5$ are shown in **Figures 7, 8**.

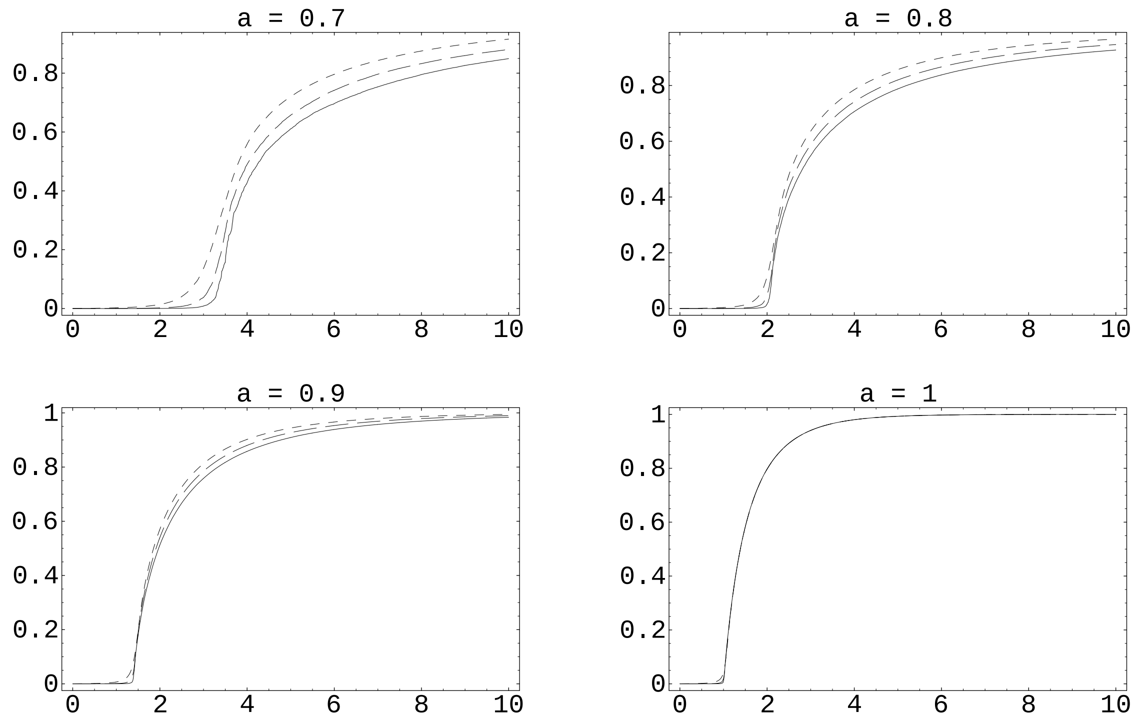

Figure 4: Largest component $\frac{M_1(t)}{N}$ for the kernel (3.18) and different N

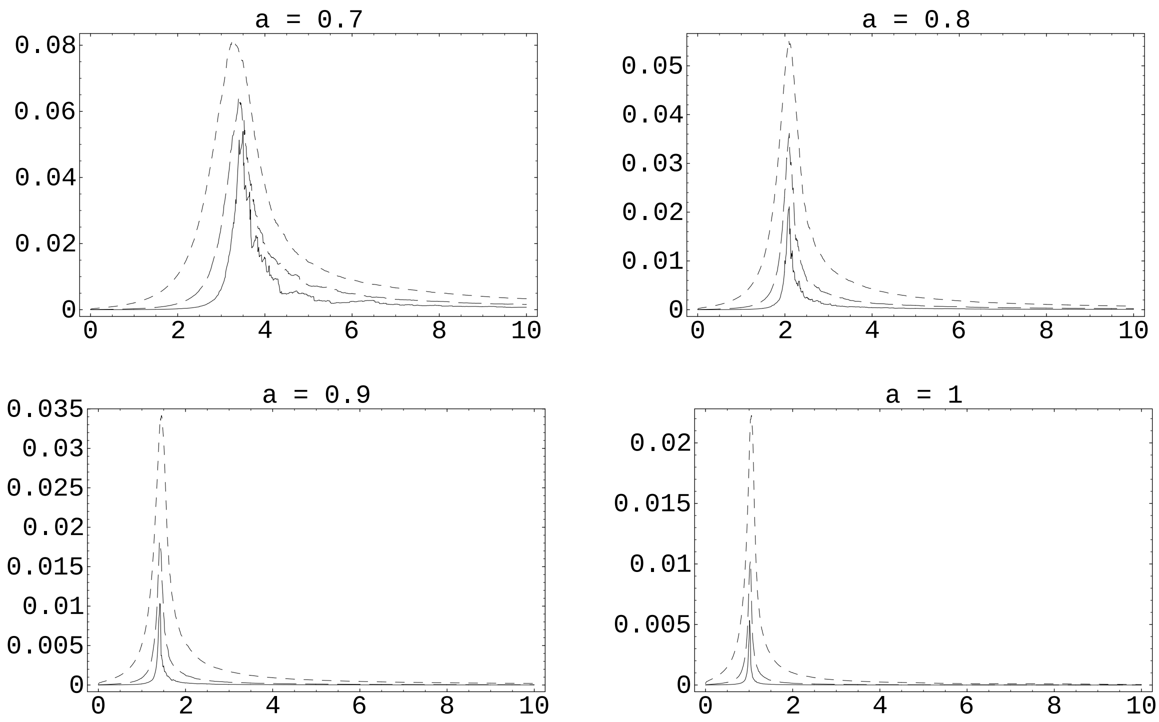

Figure 5: Second largest component $\frac{M_2(t)}{N}$ for the kernel (3.18) and different N

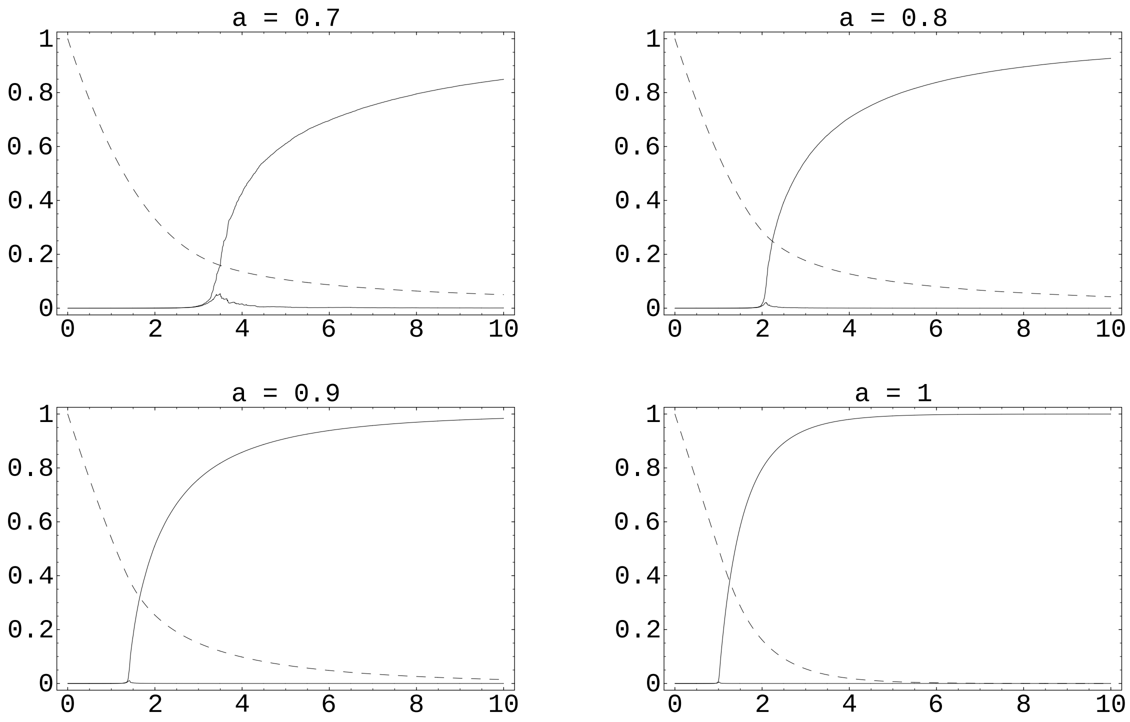

Figure 6: Two largest components and total concentration $m_0(t)$ for the kernel (3.18)

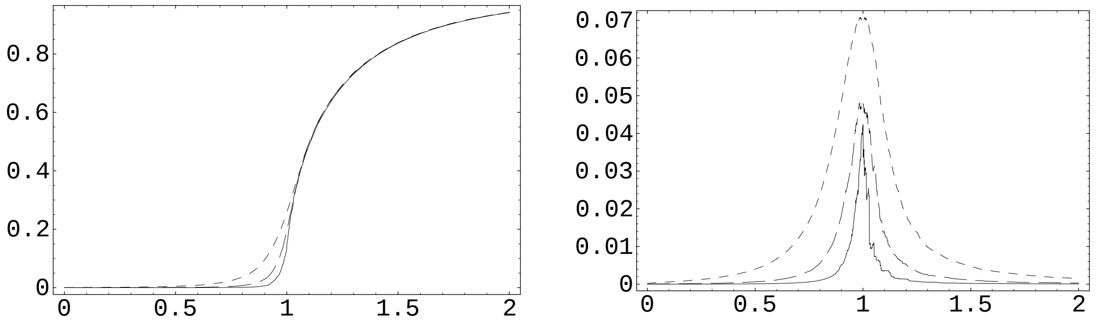

Figure 7: Largest and second largest components for the kernel (3.14) with $a = 1.5$

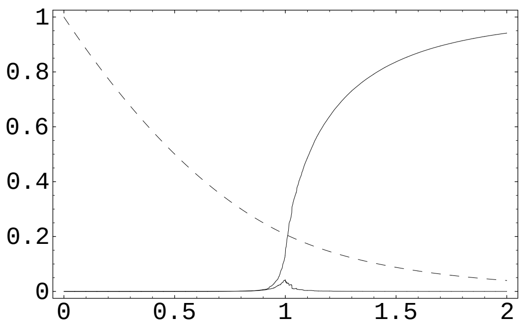

Figure 8: Two largest components and $m_0(t)$ for the kernel (3.14) with $a = 1.5$

Next we consider the **multiplicative kernel** (3.9) and the equation (cf. [21])

$$\frac{\partial}{\partial t}\,\hat{c}(t,k) \;=\; \frac{1}{2}\sum_{j=1}^{k-1} j\,(k-j)\,\hat{c}(t,j)\,\hat{c}(t,k-j) \;-\; k\,\hat{c}(t,k)\,. \tag{3.21}$$

According to (3.11), equation (1.3) coincides with equation (3.21) up to the gelation point $t_g = 1$. The unique solution of equation (3.21) is (compare with (3.10))

$$\hat{c}(t,k) \;=\; \frac{k^{k-2}}{k!}\,t^{k-1}\,\exp(-kt)\,, \qquad t \ge 0\,. \tag{3.22}$$

The total mass has the form (compare with (3.11))

$$\widehat{m}_1(t) \;=\; \begin{cases} 1\,, & \text{if} \quad 0 \le t \le 1\,, \\ \frac{t^*}{t}\,, & \text{if} \quad 1 < t\,, \end{cases} \tag{3.23}$$

where $t^* = t^*(t)$ is determined by the equation

$$t^*\,\exp(-t^*) \;=\; t\,\exp(-t)\,, \qquad t^* \in (0,1)\,, \quad t > 1\,.$$

The solution (3.22) describes the limiting behaviour (cf. [4, Cor. 1]) of the stochastic particle system beyond the gelation point. The results of the stochastic algorithm for different concentration functionals are shown in **Figure 9**. In these calculations the initial number of particles is $N = 10^6$. The exact curves for equation (3.21) are shown by solid lines, the confidence bands by dotted lines, and the curves for the Smoluchowski equation (1.3) by dashed lines. The loss of total mass (cf. (3.23)) is approximated by the largest component of the particle system (see **Figure 10**) illustrating the property

$$1 - \widehat{m}_1(t) = \lim_{N\to\infty} \frac{M_1(t)}{N}\,. \tag{3.24}$$

The confidence band is almost indistinguishable from the solid line.

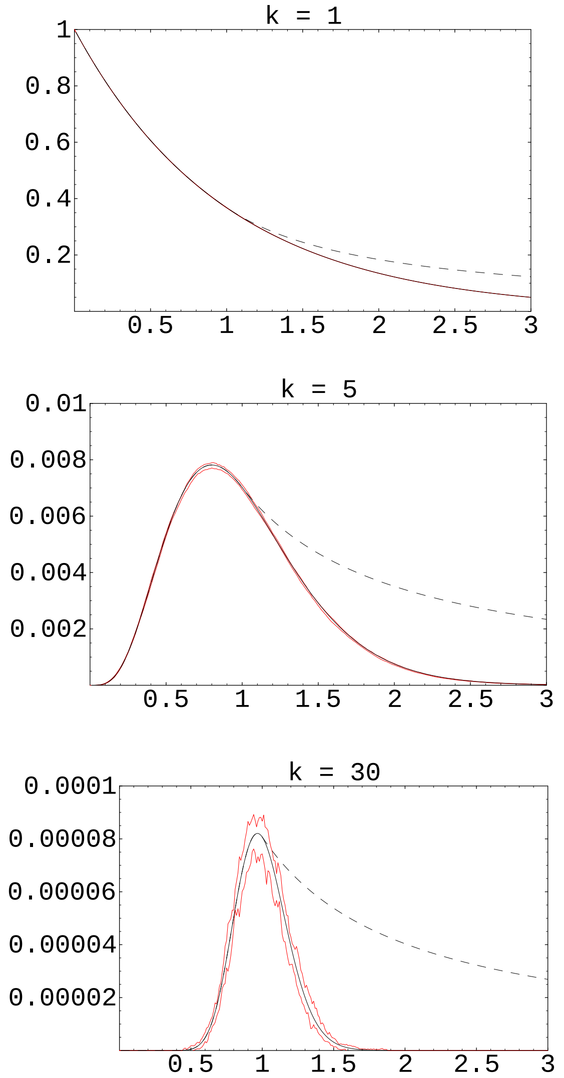

Figure 9: Solutions (3.10) (dashed) and (3.22) (solid) for the multiplicative kernel (3.9)

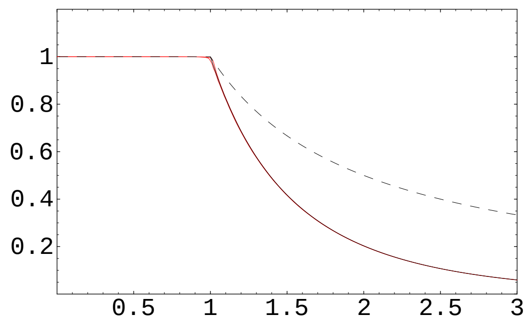

Figure 10: Functionals (3.11) (dashed) and (3.23) (solid) for the multiplicative kernel (3.9)

3.5. Efficiency

The decisive criterion for efficiency is the necessary computation time for reaching a sufficiently low error. Two basic indicators influencing the computational effort are the **number of fictitious jumps** and the **number of rejections**. The number of fictitious jumps is determined by the majorant kernel (cf. (2.9)) indicating its "quality". The number of rejections is determined by the choice of the group bounds (2.26) (cf. (2.31)). We consider the kernel (3.12) and compare the efficiency of the algorithms with two different majorant kernels. The initial number of particles is $N = 10^6$. The dashed lines correspond to the linear majorant kernel (2.20), and the solid lines to the maximum majorant kernel (2.12).

The absolute numbers of jump attempts and the relative numbers of fictitious jumps are shown in **Figure 11**. The number of jump attempts equals the number of time steps (cf. (2.13), (2.21)). The relative number of fictitious jumps is about 13% in one case and 97% in the other case at time $t = 4$. Note that the number of real jumps does not depend on the choice of the majorant kernel and can be determined from the total concentration via $N\,(1 - m_0(t))$.

In the algorithm with the maximum majorant kernel no rejections occur. The relative number of rejections for the linear majorant kernel are shown in **Figure 12**. The proportion of rejections for this algorithm is about 35% (the basis $\beta = 2$ was used). The upper bound (2.32) for the relative number of the rejections takes the form $1 - \frac{1}{\beta}$ (cf. (2.23), (2.25)).

A comparison of the CPU-time (in seconds) for both algorithms is given in **Figure 13**. There is a significant gain factor depending on the length of the time interval. Note that for gelling kernels calculations with the maximum majorant kernel (2.12) become very time consuming when approaching the gelation point.

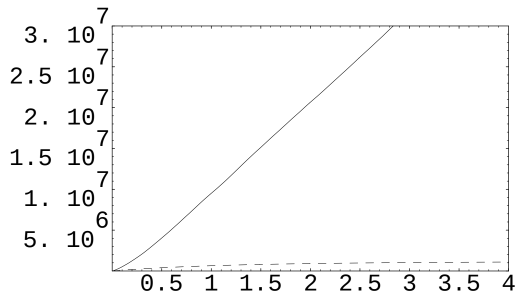

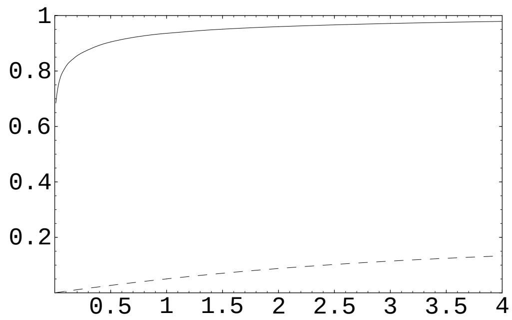

Figure 11: Number of time steps (left) and relative number of fictitious jumps (right)

4. Concluding remarks

A class of stochastic algorithms for the numerical treatment of coagulation processes was introduced. By an appropriate choice of the majorant kernel, a remarkable gain in efficiency has been achieved. This effect is mainly based on a significant reduction of

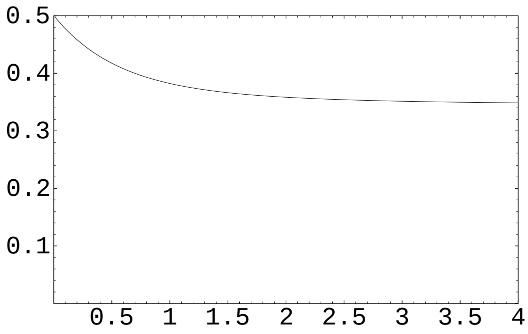

Figure 12: Rejections

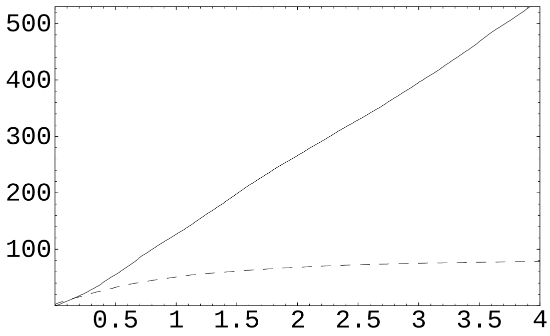

Figure 13: CPU-time

the number of fictitious jumps for systems with unbounded kernels and strongly varying cluster sizes.

The algorithm works both in the discrete and the continuous case. Generalizations to equations with fragmentation [7] and source terms are straightforward. Further improvements are possible. In particular, the rejections in the case $i = j$ (cf. (2.16), (2.17)) can be avoided, which is of some relevance in situations where large particles occur. In the discrete case it is more efficient to use the particle number representation (cf. (3.5)) instead of the particle representation (1.4) for particles with lower sizes.

The algorithm in its present form is not suitable for calculations on very long time intervals, since the number of simulation particles is strictly decreasing. There are some interesting ideas in the literature how to handle this problem. The number of particles in the system may be doubled, when necessary, by dividing each particle into two equal parts, or, more generally, particles with variable weights may be used (see [20]). An algorithm based on the mass flow instead of the particle number flow was proposed in [3]. Here the number of simulation particles is preserved. These ideas can be implemented in the framework of the new class of algorithms and will be studied in the near future.

The main practical effect of the improved efficiency of our algorithm is that it can be used as a tool for calculations up to and even beyond the gelation point. This seems to be very useful for getting some heuristical insight into the gelation phenomenon for general gelling kernels.

Rigorous convergence results for general coagulation kernels are known up to the gelation point [18]. Convergence to the solution of the Smoluchowski equation after the gelation point is expected [14] for kernels $K(i,j) = o(i)\,o(j)$. However, the case of multiplicative kernel (3.9) shows that the limiting behaviour of the stochastic particle system after the gelation point is described by an equation (cf. (3.21)) different from the Smoluchowski equation (1.3). Numerical observations illustrate the known results and confirm the hypothesis of convergence after the gelation point to some deterministic limit.

The numerical studies of the behaviour of the largest component in the particle system suggest that several properties, known for the multiplicative kernel (3.9), might be true for larger classes of gelling kernels. There are numerical indications that the quantity $\frac{M_1(t)}{N}$ converges to a deterministic limit. This limit can be used to determine the time of emergence of a cluster of order N as

$$t_g^s = \inf\left\{t > 0 \; : \; \lim_{N\to\infty} \frac{M_1(t)}{N} > 0\right\}.$$

It is of interest to find out, for which kernels $t_g^s = t_g$ holds. For the multiplicative kernel, this property is illustrated in Figure 4 ($a = 1$). For the kernel (3.14), Figure 7 provides numerical evidence for $t_g = t_g^s = 1$ (cf. [1]). The question for which kernels the limit of the normalized largest component determines (as in (3.24)) the loss of total mass of the corresponding solution is a related open problem.

Acknowledgements

This work was supported by Deutsche Forschungsgemeinschaft (Schwerpunktprogramm "Interagierende stochastische Systeme von hoher Komplexität"). The authors appreciate useful discussions with H. Babovsky, F. Guiaş and K. Sabelfeld on numerical issues related to the coagulation equation.

References

[1] D. Aldous, *Emergence of the giant component in special Marcus-Lushnikov processes*, Random Structures Algorithms, 12 (1998), pp. 179–196.

[2] D. J. Aldous, *Deterministic and stochastic models for coalescence (aggregation, coagulation): a review of the mean-field theory for probabilists*, Bernoulli, 5 (1999). To appear. See http://www.stat.berkeley.edu/users/aldous.

[3] H. Babovsky, *On a Monte Carlo scheme for Smoluchowski's coagulation equation*, Tech. Report M20/98, Technische Universität, Institut für Mathematik, Ilmenau, 1998.

[4] E. Buffet and J. V. Pulé, *Polymers and random graphs*, J. Statist. Phys., 64 (1991), pp. 87–110.

[5] Y. R. Domilovskiy, A. A. Lushnikov, and V. N. Piskurov, *Monte Carlo simulation of coagulation processes*, Izv. Acad. Sci. USSR Atmospher. Ocean. Phys., 15 (1979), pp. 129–134 (1980).

[6] R. L. Drake, *A general mathematical survey of the coagulation equation*, in Topics in Current Aerosol Research (Part 2), G. Hidy and J. Brock, eds., Pergamon Press, Oxford, 1972, pp. 201–376.

[7] A. Eibeck and W. Wagner, *Approximative solution of the coagulation-fragmentation equation by stochastic particle systems*, Tech. Report 433, Weierstraß–Institut für Angewandte Analysis und Stochastik, Berlin, 1998. To appear in Stochastic Anal. Appl.

[8] S. N. Ethier and T. G. Kurtz, *Markov processes. Characterization and convergence*, Wiley, New York, 1986.

[9] A. J. Garcia, C. Van den Broeck, M. Aertsens, and R. Serneels, *A Monte Carlo simulation of coagulation*, Phys. A, 143 (1987), pp. 535–546.

[10] D. N. Gillespie, *The stochastic coalescence model for cloud droplet growth*, J. Atmospheric Sci., 29 (1972), pp. 1496–1510.

[11] ——, *An exact method for numerically simulating the stochastic coalescence process in a cloud*, J. Atmospheric Sci., 32 (1975), pp. 1977–1989.

[12] F. Guiaş, *A Monte Carlo approach to the Smoluchowski equations*, Monte Carlo Methods Appl., 3 (1997), pp. 313–326.

[13] ——, *Coagulation-fragmentation processes: relations between finite particle models and differential equations*, Tech. Report 41, Interdisziplinäres Zentrum für wissenschaftliches Rechnen der Universität Heidelberg (SFB 359), Heidelberg, 1998.

[14] I. Jeon, *Existence of gelling solutions for coagulation-fragmentation equations*, Comm. Math. Phys., 194 (1998), pp. 541–567.

[15] N. J. Kokholm, *On Smoluchowski's coagulation equation*, J. Phys. A, 21 (1988), pp. 839–842.

[16] A. A. Lushnikov, *Some new aspects of coagulation theory*, Izv. Akad. Nauk SSSR Ser. Fiz. Atmosfer. i Okeana, 14 (1978), pp. 738–743.

[17] A. H. Marcus, *Stochastic coalescence*, Technometrics, 10 (1968), pp. 133–148.

[18] J. R. Norris, *Smoluchowski's coagulation equations: uniqueness, non-uniqueness and a hydrodynamic limit for the stochastic coalescent*, Ann. Appl. Probab., (1999). To appear. See www.statslab.cam.uk/∼james.

[19] K. K. Sabelfeld, *Stochastic models for coagulation of aerosol particles in intermittent turbulent flows*, Math. Comput. Simulation, 47 (1998), pp. 85–101.

[20] K. K. Sabelfeld, S. V. Rogazinskii, A. A. Kolodko, and A. I. Levykin, *Stochastic algorithms for solving Smoluchowski coagulation equation and applications to aerosol growth simulation*, Monte Carlo Methods Appl., 2 (1996), pp. 41–87.

[21] P. G. J. van Dongen and M. H. Ernst, *Fluctuations in coagulating systems*, J. Statist. Phys., 49 (1987), pp. 879–926.

[22] M. von Smoluchowski, *Drei Vorträge über Diffusion, Brownsche Molekularbewegung und Koagulation von Kolloidteilchen*, Phys. Z., 17 (1916), pp. 557–571, 585–599.